Supporting Information

Photoacoustic Induced Surface Acoustic Wave Sensor for Concurrent Optical-Mechanical Microfluidic Sensing of Dyes and Plasmonic Nanoparticles

Rahul Kishor,[a,b,c†] Fei Gao,[c†] Sivaramapanicker Sreejith,[d†] Xiaohua Feng,[c] Yen Peng Seah,[e] Zhenfeng Wang,[e] Mihaiela C. Stuparu,[d,f] T. T. Lim,[g] Xiaodong Chen[f] and Yuanjin Zheng[c*]

[a] Environmental Chemistry and Materials Group, Nanyang Environment & Water Research Institute (NEWRI), Nanyang Technological University, 1 Cleantech Loop, Singapore 637141

[b] Interdisciplinary graduate school (IGS), 50 Nanyang Avenue, Nanyang Technological University, Singapore 639798

[c] Division of Circuits and Systems, School of Electrical and Electronic Engineering, Nanyang Technological University, 50 Nanyang Avenue, Singapore 639798.

[d] Division of Chemistry and Biological Chemistry, School of Physical and Mathematical Sciences, Nanyang Technological University, 21 Nanyang Link, 637371, Singapore 637371

[e] Singapore Institute of Manufacturing Technology, 71 Nanyang Drive, Singapore 638075

[f] School of Materials Science and Engineering, Nanyang Technological University, 50 Nanyang Avenue, 639798, Singapore.

[g] Division of Environmental and Water Resources Engineering, School of Civil and Environmental Engineering, Nanyang Technological University, 50 Nanyang Avenue, Singapore 639798

[†] These authors contributed equally to this work.

* Fax: (+65)67933318; Tel: (+65)65927764; E-mail: YJZHENG@ntu.edu.sg

S1. Device and experimental details

S1.1 SAW device design:

Table.1 SAW-IDT design parameters

Parameter	Values
IDT width (λ/8 in μm)	37.5
Number of IDT pairs	25
IDT thickness (nm)	150
Aperture (mm)	4

The IDT width (d) is the design parameter used for generating a specific frequency SAW. The split-finger configuration has an IDT width equal to λ/8, where λ is the SAW wavelength.

$$d = v/8f_o \quad \backslash * \text{MERGEFORMAT (1)}$$

where "v" is the velocity of the surface acoustic wave and "f_o" is the desired SAW frequency. For 128° YX $LiNb0_3$ substrate, the SAW velocity "v" is 3979 m/s.[1]

S1.2 SAW device fabrication:

The SAW device was fabricated using a two-step optical lithographic process. The fabrication process of the SAW device begins with a layer of aluminium patterned (thickness of 150 nm) on the 4 inch 128^0 rotated Y cut $LiNbO_3$ substrate using a positive photoresist to form the inter-digital transducer (IDT).The electrodes has a separation (d) and width (d) of 37.5 μm. The metal pad has a dimension of 3.5 mm (length) x 3.5 mm (width) and 500 nm (thickness). Figure S1 shows the steps involved in the SAW device fabrication. The critical dimension (CD) in step 4 and step 8 depends on the metal IDT width (37.5 μm) and metal pad length/width (3.5 mm) respectively.

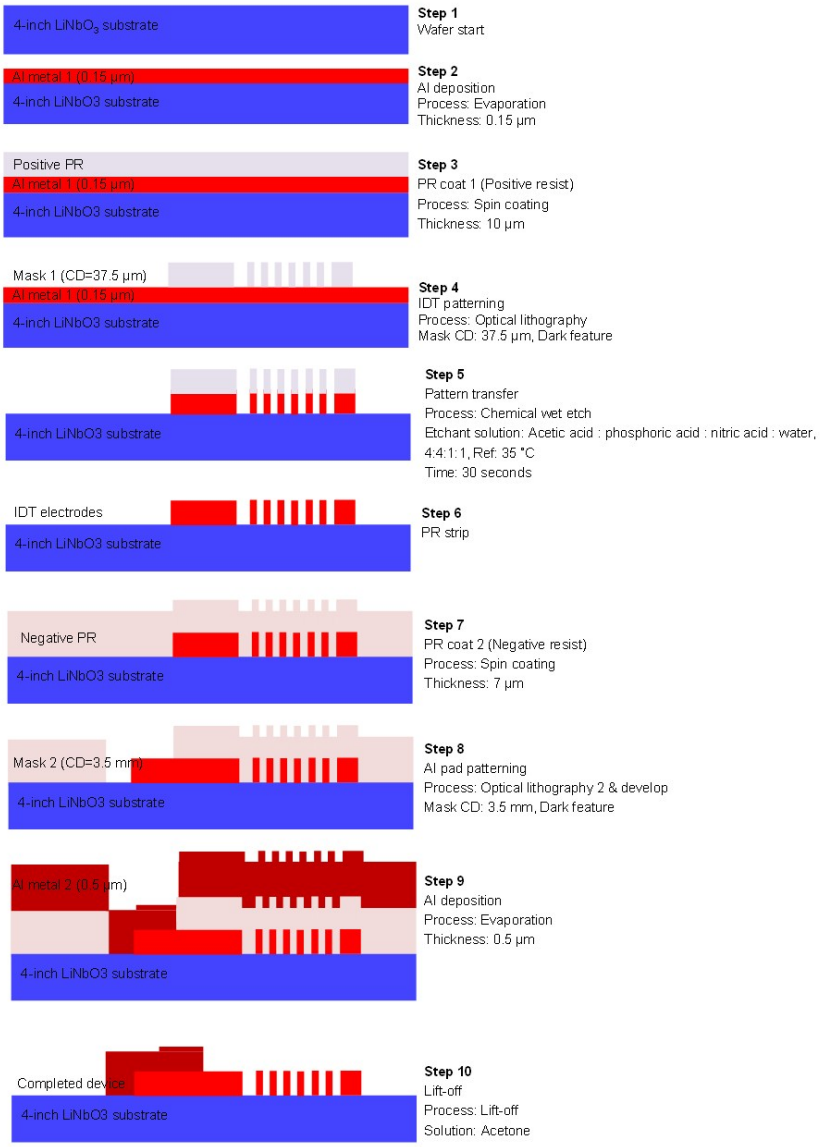

Figure S1. SAW fabrication process.

S1.3 SAW device characterization:

The frequency response of the fabricated device measured using the E5061B ENA Series Network Analyzer is shown in Figure S2. The resonant frequency of the device is at 12.9 MHz.

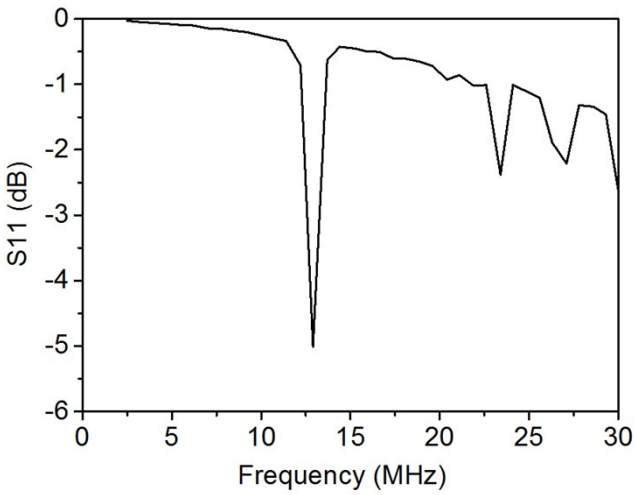

Figure S2. Frequency response (S11) of the SAW device measured using the network analyzer. The resonant frequency of the device is 12.9 MHz.

S1.4 PDMS microfluidic channel and dimensions:

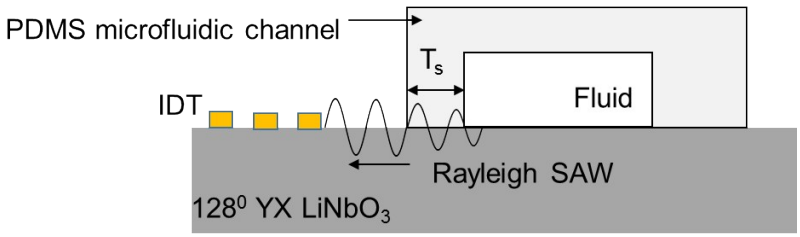

Figure S3. Schematic illustration of the PDMS microfluidic channel on the SAW substrate, where Ts denotes the side wall thickness.

S1.5 Experimental configuration:

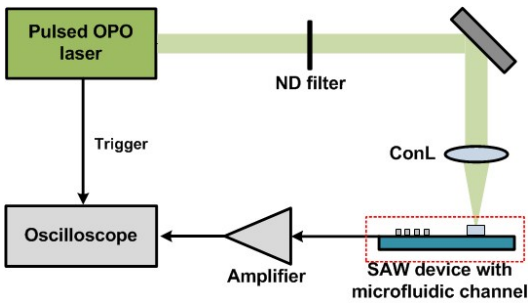

Figure S4. The experimental setup for PA measurement using the proposed SAW-PA sensor. OPO: optical parametric oscillator; ND: neutral density; ConL: condenser lens; IDT: interdigital transducer

The experiment involved exciting the sample liquids with wavelength from visible to near-infrared wavelengths, the RMS10X-PF (Olympus) was selected which works in the visible and near infra-red wavelength.

S2. Analytical study of the PA-SAW mode conversion:

The generated PA is converted to leaky SAW beneath the microchannel, which is then converted into a SAW at the edge of the microchannel. The principle of the mode conversion process involved in exciting a SAW is shown in Figure S5. The conversion from leaky wave to surface wave will be 100 percent efficient, if we assume that the substrate fields of the leaky and surface wave are similar.[2] The generated PA signal inside the liquid is a longitudinal wave. The conversion process is equivalent to the excitation of the Rayleigh wave by a wedge transducer as mentioned in a previous publication.[3] A Rayleigh wave is excited on the substrate if it satisfies the condition that c_R ,the Rayleigh wave velocity in the substrate (3979 m/s) [1], should be greater than c_W, the longitudinal wave velocity in the liquid (1500 m/s in water). This condition is satisfied in our configuration.

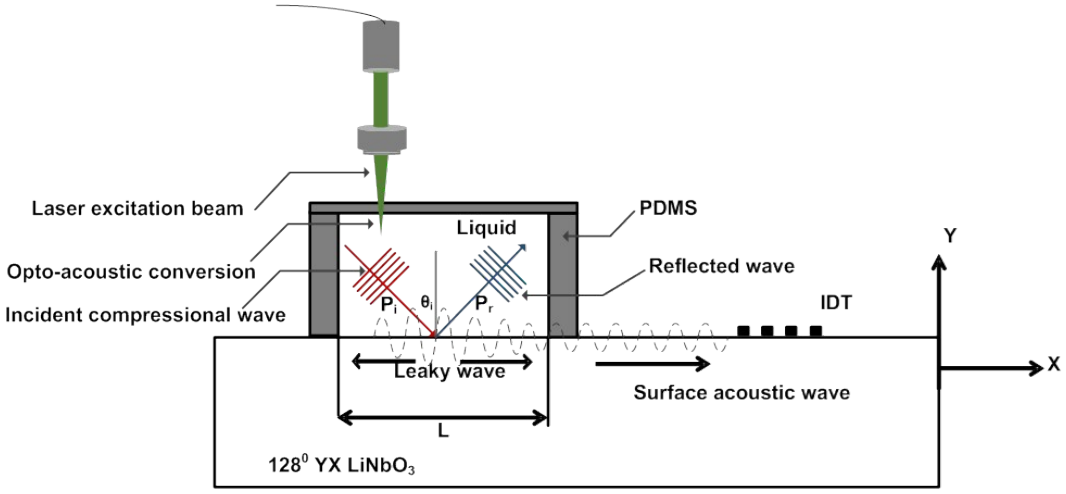

Figure S5. Schematic representation of the mode conversion process in generating a Rayleigh surface acoustic wave excitation triggered by the photoacoustic waves. P_i, P_r and θ_i refer to the incident pressure, reflected pressure and angle of incidence respectively.

All the longitudinal waves inclined at an angle θ_i greater than the critical angle defined by:

$\sin\theta_i = c_W / c_R$, satisfies the criteria to excite the Rayleigh wave. The efficiency of the conversion process from the longitudinal to the leaky surface wave is calculated analytically by the equation [3, 4]:

$\eta_0 = 2[1-\exp(-\alpha L]^2 / \alpha L$. *
MERGEFORMAT (2)

where α denotes the leak rate or attenuation per unit length of the surface acoustic wave under the microchannel, which is a function of the frequency of the wave, acoustic impedance in the liquid and

the ratio of mode displacement to the power flow. L denotes the aperture or the length on the substrate where the longitudinal wave strikes. Fraser *et.al* [3] plots the efficiency with respect to the factor αL and shows that a conversion efficiency of 81% is obtained in the mode conversion process. High conversion efficiency of 81% percent proves the significance of using the SAW as a detector of the longitudinal PA signal.

S3. Experimental results:

S3.1 SAW-PA signal generated by the PDMS microfluidic channel at different optical wavelengths:

The influence of PDMS on the SAW-PA signal generated by the fluid samples was analyzed. Figure S6 shows the background signal generated by the PDMS microfluidic channel for different optical wavelengths. The background signal intensity is maximum in the blue spectral region.

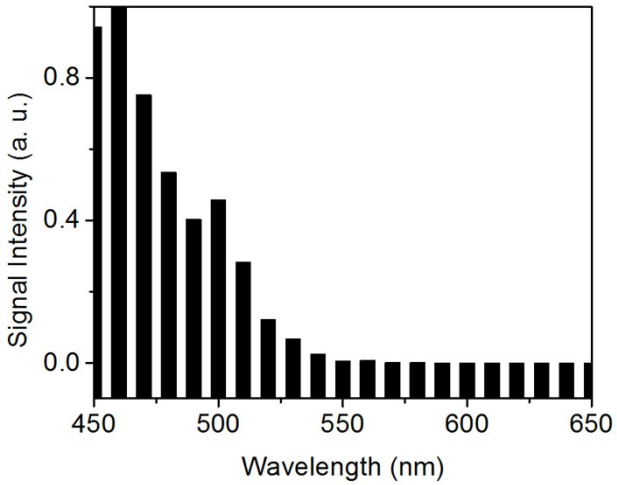

Figure S6. Background SAW-PA signal intensity generated by the PDMS microfluidic channel for different optical excitation wavelengths.

S3.2 PSD spectra of the transient signal obtained from the dye:

Figure S7 shows the PSD spectra of the transient signals obtained for the erythrosine dye (Figure 3a) from 2-4 μs (red curve) and 6-8 μs (black curve). The spectra shows a dominant frequency component at 12.9 MHz, which coincides with the SAW resonant frequency.

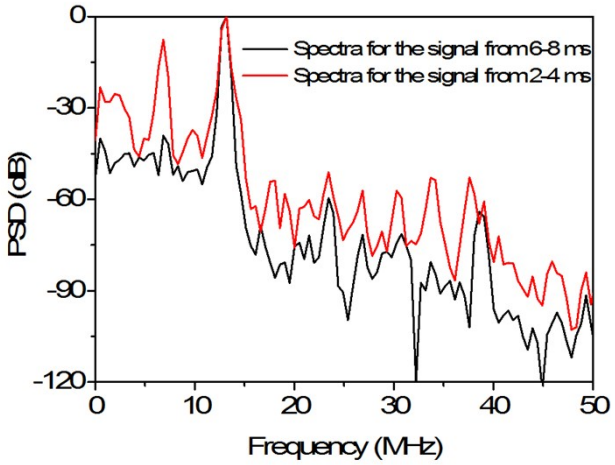

Figure S7. Results of the power spectral density (PSD) analysis for specific durations (2-4 μs and 6-8 μs) of the transient signal displaying the dominant frequency component at 12.9 MHz.

S3.3 Repeatability of the transient data:

To illustrate the repeatability on the transient data shown in Figure 3a, we provide a set of time domain data obtained for erythrosine dye solutions of various concentrations (75, 50 and 25 % volume concentrations each) and also calculated the cross-correlation between the transient signals to highlight the robustness of the signal. The repeatability can be estimated by correlation analysis.[5]

- Time domain data obtained for various concentrations are shown below:

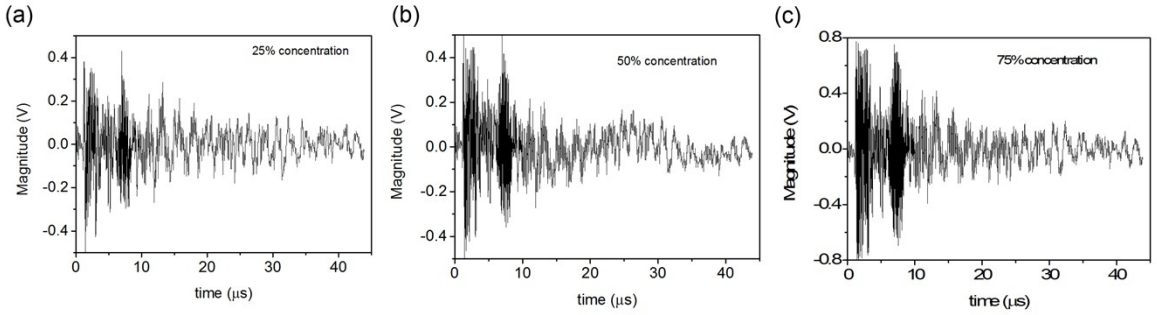

Figure S8. Repeatability of the data: Transient signals obtained for various erythrosine dye concentrations: a) 25%, b) 50% and c) 75%.

- The Pearson's linear correlation coefficients for the transient signals obtained for the signals s1 and s2 in Figure A is 0.816, and for signals s2 and s3 is 0.904. A value greater than +0.7 indicate very high correlation between signals. Hence, the transient data is repeatable

S3.4 SAW-PA response from various concentrations of GNR solutions:

Fig. S9 shows the SAW-PA response normalized on laser intensity and peak amplitude for different concentrations of gold nanorods solution at optical wavelength of 532 nm and 1064 nm. The gold nanorods of dimension 10 nm x 85 nm, with the transverse and longitudinal plasmon resonance modes at 512 nm and 1064 nm respectively were used for the study.

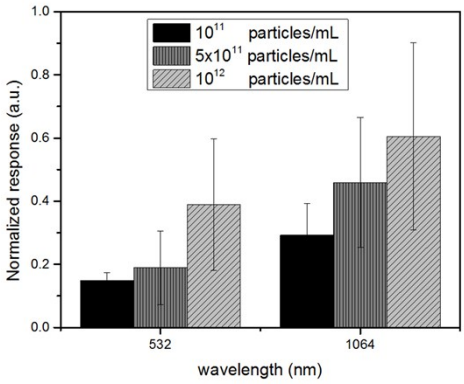

Figure S9. SAW-PA response of the gold nanorods (10 nm x 85 nm) at 532 nm and 1064 nm for different concentrations.

S3.5 TEM images of the gold nanoparticle and gold nanorods

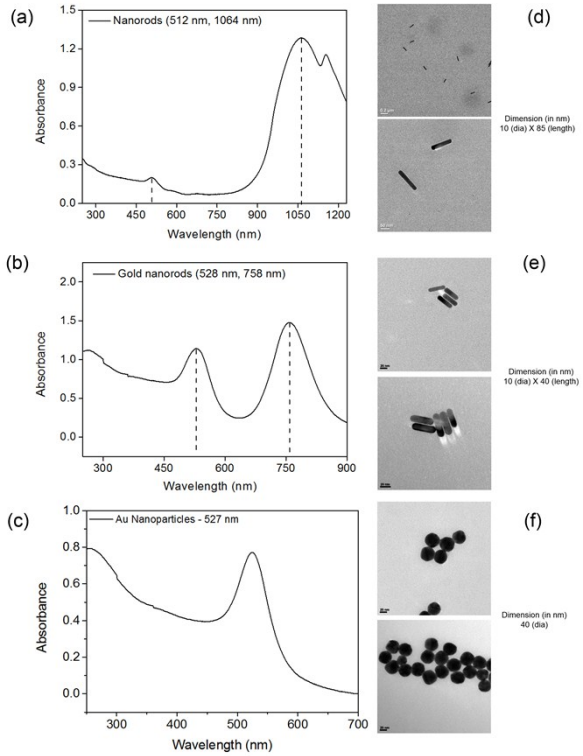

Figure S10. UV-Vis absorption spectra and TEM images of the gold nanostructures. (a),(b) and (c) represents the UV-Vis absorption spectrum of the 10 nm × 85 nm gold nanorod, 10 nm × 40 nm gold nanorod and 40 nm gold nanoparticle respectively. (d), (e) and (f) represents the TEM images of the corresponding nanostructures.

S3.6 Sensing mechanisms for different morphology of gold nanostructures using SAW-PA device

The plasmon resonance wavelength depends on the various parameters including: the size, shape, material composition, surface coating and medium. Each of these parameters can be tuned to vary the surface plasmon resonance wavelength. By changing the dimension of the gold nanorods from 10 nm × 40 nm to 10 nm × 85 nm, the longitudinal resonance shifts from 758 nm to 1064 nm as shown in Fig.S10. The effect of shape is understood by comparing the single resonance peak for the GNP and two resonance peaks- transverse and longitudinal resonance modes for the GNRs. The transverse mode resonance is coincident with the plasmon resonance of GNP, while the longitudinal resonance at higher wavelengths depends on the aspect ratio of the nanorods.[6]

According to Gans theory[7], the extinction coefficient (proportional to the optical absorption) for N particles of volume V is given by:

$$\kappa = \frac{2\pi NV\varepsilon_m^{3/2}}{3\lambda}\sum_j \frac{(1/P_j^2)\varepsilon_2}{\left(\varepsilon_1 + \frac{1-P_j}{P_j}\varepsilon_m\right)^2 + \varepsilon_2^2} \quad \backslash*$$

MERGEFORMAT (3)

where ε_m is the medium dielectric constant, ε_1 and ε_2 represent the real and imaginary parts of the material dielectric function, P_j values are the depolarization factors.

The absorption spectra peak for the longitudinal plasmon resonance mode calculated for a gold nanorod with aspect ratio R is given by[6]

$$\lambda_{\max} = (33.34R - 46.31)\varepsilon_m + 472.31 \quad \backslash*$$

MERGEFORMAT (4)

Thus the changing aspect ratio shifts the absorption peak wavelength, which is determined by measuring the optical wavelength at which the SAW-PA response is the maximum. Fig. S11 shows the schematic of the sensing mechanism for different morphology of gold nanostructures, with their corresponding resonance modes.

Fig. S11 shows the schematic representation of the sensing mechanism for different morphology of gold nanostructures using the SAW-PA device. The absorption spectra shows peaks at: 527 nm for the GNP, the two GNR's selected has a transverse plasmon absorption peak at 512 nm and 528 nm and corresponding longitudinal peaks at 1064 nm and 758 nm. A nanosecond pulsed laser of a certain wavelength matches the frequency of oscillation of the electron cloud in the gold nanostructure and the plasmon resonance occurs and light is absorbed. The heat generated due to absorption is rapidly

transferred to the surrounding media at a heat transition time which is much shorter than the pulse width (5-10 ns).[8, 9] The surrounding medium (water) undergoes thermal expansion due to the heat transfer, which generates a longitudinal pressure wave inside the microfluidic channel. The longitudinal acoustic wave is mode-converted to a SAW.

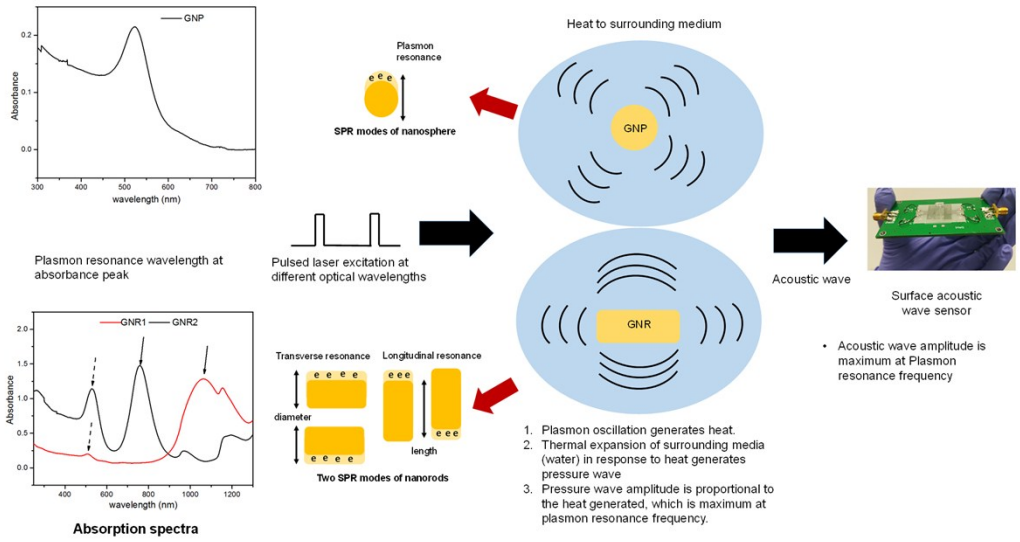

Figure S11. Schematic diagram on the sensing mechanism for different morphology of gold nanostructures. The absorption spectra peaks corresponds to the surface plasmon resonance wavelength. The dashed and straight points to the transverse resonance and longitudinal resonance wavelength respectively of the GNRs of dimension 10 nm × 85 nm (GNR1) and 10 nm × 40 nm (GNR2) (diameter × length).

Reference:

1. D. P. Morgan, *Surface acoustic wave filters with applications to electronic communications and signal processing*, Academic Press, Amsterdam, 2nd edn., 2007.
2. H. L. Bertoni and T. Tamir, *IEEE Trans. Sonics Ultrason.*, 1975, **22**, 415-420.
3. J. Fraser, B. T. Khuri Yakub and G. S. Kino, *Appl. Phys. Lett.*, 1978, **32**, 698-700.
4. X. Jia, *J. Acoust. Soc. Am*, 1997, **101**, 834-842.
5. S. Nakagawa and H. Schielzeth, *Biological Reviews*, 2010, **85**, 935-956.
6. S. Link and M. A. El-Sayed, *J Phys Chem B.*, 1999, **103**, 8410-8426.
7. R. Gans, *Ann. Phys.* , 1915, **47**, 270.
8. G. V. Hartland, *Chem. Rev.*, 2011, **111**, 3858-3887.
9. V. K. Pustovalov, *Chem. Phys.*, 2005, **308**, 103-108.